Evolutionary behaviour of miniemulsion phases: I. Hard sphere interaction and bound water on miniemulsion droplets

2000 J. Phys.: Condens. Matter 12 249

(http://iopscience.iop.org/0953-8984/12/3/304)

J. Phys.: Condens. Matter **12** (2000) 249–264. Printed in the UK PII: S0953-8984(00)04308-3

Evolutionary behaviour of miniemulsion phases: I. Hard sphere interaction and bound water on miniemulsion droplets

Yukiteru Katsumoto†, Hideharu Ushiki†, Alain Graciaa‡ and Jean Lachaise‡

† Laboratory of Transport and Transformation in Bio-Systems, Department of Bio-Mechanics and Intelligent Systems, Graduate School of Bio-Applications and Systems Engineering (BASE), Tokyo University of Agriculture and Technology, 3-5-8, Saiwai-cho, Fuchu-shi, 183-8509 Tokyo, Japan

‡ Laboratoire de Thermodynamique des Etats Métastables et de Physique Moléculaire, Université de Pau et des Pays de l'Adour, 64000 Pau, France

E-mail: yukiteru@cc.tuat.ac.jp

Received 21 May 1999, in final form 3 September 1999

Abstract. The interaction between nano sphere droplets in translucent oil in water (O/W) emulsion phases, so-called miniemulsion phases, was investigated by using light scattering measurement techniques. We choose the ternary system of water/hexadecane/Mergital LT7 (the main component is heptaethylene glycol mono-*n*-dodecyl ether). Rayleigh ratio measurement was performed with changing dispersed phase volume fraction ϕ', and it revealed the fact that the osmotic compressibility is in good agreement with that of a hard sphere fluid. The dependence of the collective diffusion coefficients, measured by dynamic light scattering experiments, is similar to those observed in colloidal hard sphere suspensions. We found out that the ratio of the hydrodynamic diameter to the hard sphere diameter is 1.19 and the volume fraction of dispersed droplets is given by $\phi = 1.35\phi'$. Preparing miniemulsions with various water to oil ratios, it was revealed that the ratio ϕ/ϕ' was varied from 1.01 to 1.33. This indicates that the underestimation of the total volume of droplets calculated by the sum of surfactant and oil volume was not negligible. It is therefore considered that the volume fraction of bound water on miniemulsion droplets should be taken into account. We briefly discuss the idea that bound water plays an important role in obtaining a homogeneous miniemulsion phase.

1. Introduction

Emulsions are widely used in industrial processes such as waste water treatment, mineral recovery, paper manufacturing, foods and cosmetic industries, biotechnical and biomedical tools. During the last decades, formation mechanisms and break-down processes of emulsions have been studied experimentally and theoretically [1].

Recently, we have been interested in the emulsion system considered as a curious domain in complex physics. In such a system, we expect that one can study basically morphological formation [2]. Also, we will be able to develop new ideas and thoughts for studying a system that has many components and shows many states or phases [3]. For instance, it is well known that a ternary system of oil/water/nonionic surfactant shows diverse phases such as hexagonal, cubic, lamellar liquid crystal, spherical droplets and inverted ones [4]. The interactions of only three components allow the above-mentioned system to show these intricate and various forms. We expect that such a system gives us an excellent sample for investigating morphological

0953-8984/00/030249+16$30.00

formations. We concentrate first on elucidating the evolutionary behaviour of the oil in water (O/W) emulsion phase in a ternary system of oil/water/nonionic surfactant in this series of papers, namely 'Evolutionary behaviour of miniemulsion phases'.

In general, emulsion phases are thermodynamically unstable, because they include a very large interface. D.L.V.O. theory gives an important comprehension of the stability of emulsions that have charged interfaces. It explains that the balance of the electrostatic repulsive force and London–van der Waals force decides the interaction of dispersed particles. But it is difficult to explain the stability of emulsions involving nonionic surfactants applying D.L.V.O. theory. In these cases, we must consider the steric repulsive force between dispersed particles. There are several reports that have pointed out the importance of this kind of interaction force [5–7]. In these reports, an important role of solvation of the hydrophilic head group of nonionic surfactants was suggested. But there are still many unsolved problems related to the steric stabilization in emulsion systems. For instance, this is not only concerned with their compositions, but also are dependent on the technique for emulsification. So it is desirable to study the interaction between emulsion droplets for clarifying the stabilization mechanism of emulsions.

In the previous reports [8, 9], we proposed a thermal protocol that has allowed us to produce translucent O/W (oil in water) emulsions consisting of nano-sphere droplets. In spite of the fact that these droplets had a much smaller diameter (about 30 nm), this O/W emulsion is not a microemulsion, i.e. this phase is a thermodynamically metastable. As a matter of course, this emulsion phase evolves to a thermodynamically stable one (in this case it will be Winsor's type I). Hence we consider this emulsion phase one of the miniemulsion phases.

In these systems, the interaction between emulsion droplets can be investigated experimentally by measuring the light scattering of the dispersion. Because the size of miniemulsion droplets is small with respect to the wavelength of the incident light used, the light scattering gives a direct measurements of a hard sphere interaction potential existing between these droplets in terms of Percus–Yevick approximation [10] for hard sphere fluid theory. Many researchers have applied this measurement technique in microemulsion [11–14].

In this report, we have chosen the ternary system of brine/ethyl oleate/Eumulgin O10 and water/hexadecane/Mergital LT7. Using the PIT (phase inversion temperature) method, we can obtain a miniemulsion phase in these two systems. In order to find a way to prepare a homogeneous translucent emulsion, we choose the former system. In this system we can determine a PIT exactly by using electric conductivity measurements. We investigate the relationship between the method of preparation of miniemulsion and the physical properties of obtained miniemulsions using dynamic light scattering measurements. Then we determine a thermal protocol for obtaining a homogeneous translucent O/W emulsion.

The main point of this paper is to discuss the hard sphere interaction between O/W miniemulsion droplets using light scattering techniques. In the latter system, we can discuss the droplet interaction avoiding the effect of electrolytes in the dispersion medium. Also, we briefly discuss a role of bound water for the formation of homogeneous O/W miniemulsion droplets.

2. Experiment

2.1. Sample preparation

Miniemulsions presented in this paper are ternary systems of brine/ethyl oleate/Eumulgin O10 (the main components are decaethylene glycol mono-*n*-hexadecyl ether and decaethylene glycol mono-*n*-octadecyl ether, $C_{16}EO_{10}$ and $C_{16}EO_{10}$) and water/hexadecane/Mergital LT7

(the main component is heptaethylene glycol mono-*n*-dodecyl ether, $C_{12}EO_7$). The brine is prepared from distilled water and sodium chloride (1 M). Ethyl oleate and hexadecane were purchased from Fluka. Eumulgin O10 and Mergital LT7 were graciously furnished by Sidobre Sinnova. All materials were used without further purification. Using the PIT (phase inversion temperature) method proposed by Shinoda and Saito [15], miniemulsion is prepared by a thermal protocol under gentle agitation. The samples, which have been maintained under a temperature of 25 °C, are diluted by the dispersion medium (brine or water) about 30 minutes before each measurement.

2.2. Light scattering measurements

Relative scattering intensity and dynamic light scattering measurements were performed by using a device which is made of an He–Ne laser ($\lambda = 632.8$ nm) of 15 mW, a photon counting photomultiplier and a Malvern 7032 Multi-8 with 64 channels as the digital correlator. Measurements of Rayleigh ratio were carried out with a DLS-7000 (Otsuka). All measurements are performed at a temperature of 25 °C.

Dynamic light scattering measurements were performed by the homodyne method at scattering angles from 30° to 130°. The relationship between the normalized first-order electric field autocorrelation function $g^{(1)}(q,\tau)$ and the single-clipped, photoelectron-count autocorrelation function $G_k^2(q,\tau)$ is represented by [16]

$$G_k^{(2)}(q,\tau) = B\left(1 + \beta|g^{(1)}(q,\tau)|^2\right) \tag{1}$$

where q is the scattering vector $q = (4\pi n_0/\lambda)\sin(\theta/2)$, and β is the coherent factor which is dependent on instrumental conditions. We employed the method of cumulants [17] in order to analyse the obtained $g^{(1)}(q,\tau)$. Note that the relative scattering intensity can be estimated by the base line B of $G_k^2(q,\tau)$ as $B \propto I^{rel}(q)^2$ [17]. In the method of cumulants, $g^{(1)}(q,\tau)$ is represented by

$$\ln|g^{(1)}(q,\tau)| = -K_1\tau + \frac{1}{2!}K_2\tau^2 - \frac{1}{3!}K_3\tau^3 + \cdots \tag{2}$$

where K_m is the mth cumulant. The first cumulant is concerned with the z-averaged diffusion coefficient, $D_z = K_1/q^2$, so we can estimate the z-averaged hydrodynamic diameter a_z using the Stokes–Einstein relation as follows.

$$a_z = \frac{kT}{3\pi\eta D_z} \tag{3}$$

where η is the viscosity of the dispersion medium. The normalized second cumulant K_2/K_1^2 is related to the variance of the distribution, and the third one is a measure of the skewness or asymmetry of the distribution.

At a high volume fraction of the dispersion phase, the measured autocorrelation functions deviated from a single exponential. According to Pusey *et al* [18], the autocorrelation function should be composed of two independent modes for relatively high volume fractions and fairly narrow distribution. In this case, the $g^{(1)}(q,\tau)$ was analysed by using a double exponential function

$$g^{(1)}(q,\tau) = A_f\exp(-D_f q^2\tau) + A_s\exp(-D_s q^2\tau) \tag{4}$$

where D_f and D_s are the diffusion coefficients for the faster decaying mode and the slower decaying mode.

We wrote a program for the method of cumulants using PASCAL language (Borland: Turbo PASCAL) based on a quasi-Marquardt algorithm with a non-linear least squares method [19]. These calculations were carried out on a personal computer (PC-9821Xn). In this program, we use equation (2) including the terms up to the third order.

3. Results and discussion

3.1. The role of phase inversion temperature for preparation of homogeneous miniemulsion phases

First it is desirable to clarify the role of PIT for obtaining a homogeneous miniemulsion. We can determine exactly a phase inversion temperature (PIT) by electric conductivity measurements when we use brine as the dispersion medium [8]. Thus the ternary system of brine/ethyl oleate/Eumulgin O10 is chosen. The volume ratio of water to oil (WOR) is equal to 5 and the surfactant mass fraction is equal to 0.12.

Emulsions were prepared by a thermal protocol [8] with diverse initial temperatures varied from PIT + 9 °C to PIT − 2 °C. We obtained a translucent phase when we chose a higher temperature than the PIT. According to electric conductivity measurements, the continuous phase or dispersion medium of the obtained translucent emulsion is brine. Figure 1 shows the effect of the initial temperature on the z-averaged hydrodynamic diameter a_z and the normalized second cumulant K_2/K_1^2 of the obtained O/W emulsions. Note that we impose the dispersed phase volume fraction of 0.01 in order to accomplish these measurements under the conditions of infinite dilution. The minimum value of a_z was observed at the PIT as Shinoda and Arai proposed [20]. On the other hand K_2/K_1^2 values shows a significant difference between the regions separated by the PIT. In general, it is hard to derive accurate values for K_m ($m \geqslant 2$) by the method of cumulants because of noise on measured autocorrelation functions. We could not therefore consider that the K_2/K_1^2 value indicates directly a variance of the distribution of the obtained O/W emulsion. The great difference in K_2/K_1^2 values between two regions is enough to consider that the distribution of the obtained emulsion is very different. Thus it is concluded that we must choose an initial temperature higher than the PIT in order to obtain a homogeneous O/W emulsion phase or that with a narrow distribution, the so-called 'miniemulsion phase'.

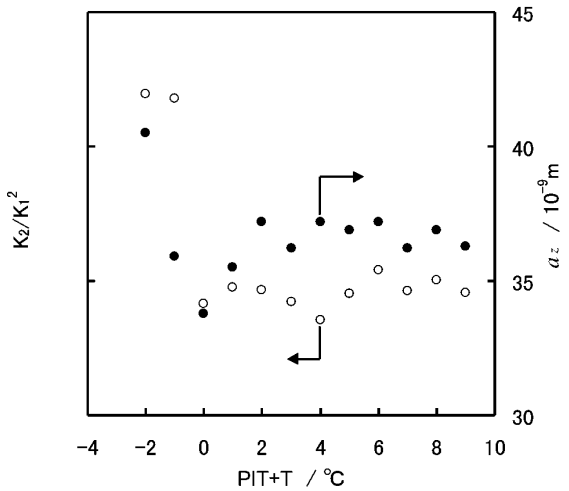

Figure 1. The z-averaged hydrodynamic a_z and the normalized second cumulant K_2/K_1^2 as a function of the preparation temperature. The filled circles (●) and the open circles (○) indicate a_z and K_2/K_1^2 respectively.

3.2. Hard sphere interaction between miniemulsion droplets

In the system mentioned in the previous section, we cannot discuss the droplet interaction without the effects of electrolytes (sodium salt) in a dispersion medium. For study of the interactions between miniemulsion droplets, therefore, we adopted the ternary system of water/hexadecane/Mergital LT7. We adopted the optimal thermal protocol described in the preceding section, which permits us to obtain a miniemulsion phase with a narrow size distribution. In this section, WOR and the weight fraction of surfactant are fixed at 8 and 0.12, respectively.

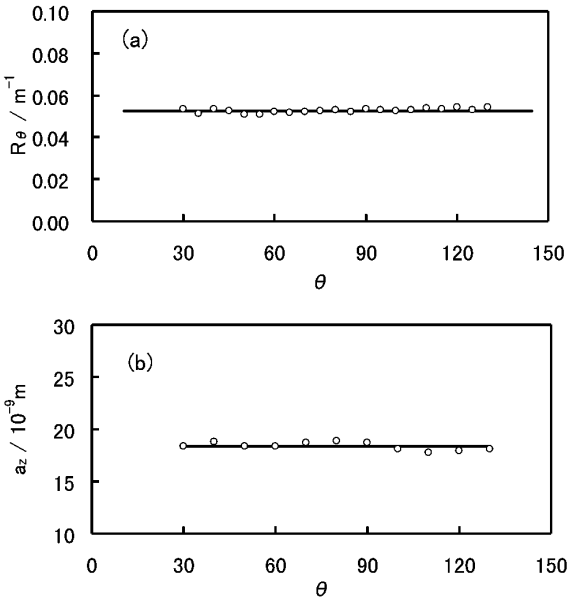

Figure 2. (a) Variation of R_θ with θ at $\phi' = 3.7 \times 10^{-3}$ for water/hexadecane/Mergital LT7 miniemulsion, of which WOR is equal to 8 and the weight fraction of surfactant is 0.12. θ was varied from 30° to 130°. The circles (○) are the measured R_θ and the solid line represents the mean value. (b) The angular dependence of a_z obtained from dynamic light scattering measurement at scattering angles from 30° to 130°. The circles (○) are the measured a_z and the solid line represents the mean value.

Figure 2(a) shows the obtained excess Rayleigh ratios R_θ with the scattering angle θ from 30° to 130°. The dispersed phase volume fraction ϕ' is fixed at $\phi' = 3.7 \times 10^{-3}$ and it is estimated by the fraction of oil and surfactant volume (V_o and V_s) to the total volume as follows

$$\phi' = \frac{V_o + V_s}{V_o + V_s + V_w} \tag{5}$$

where V_w is the variation fraction of water. R_θ values were corrected by the solvent scattered intensity measured independently. As a result, we found a slight dependence of R_θ on θ. Furthermore, we checked that there is no angular dependence on R_θ at high volume fraction ϕ'. The z-averaged hydrodynamic diameters a_z of miniemulsion droplets were measured independently, and figure 2(b) shows the angular dependence of a_z. The obtained a_z varied from 17.9 to 18.9 nm, and the mean value was 18.4 nm. Here again, we can find that there is no angular dependence of a_z. It is worth noting that we monitored a_z for 6 hours and the obtained a_z did not change significantly.

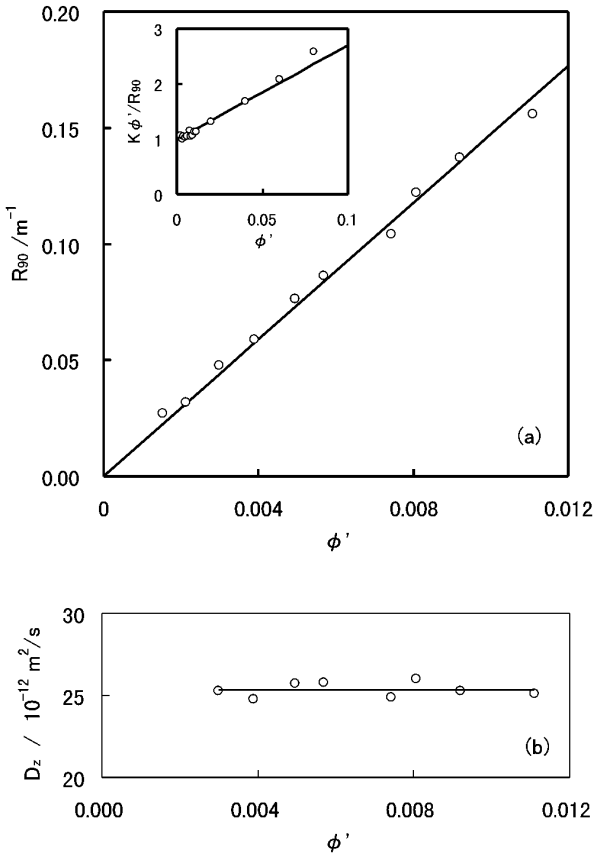

Figure 3. (a) Dependence of Rayleigh ratio R_{90} on ϕ'. The scattering angle is fixed at 90°, and ϕ' is varied from 1.52×10^{-3} to 1.11×10^{-2}. The circles (○) are the measured R_{90}; the solid line was calculated with equation (12) substituting $n_s = n_0 + 0.112\phi$ and $\phi = 1.35\phi'$ with $a = 15.5$ nm. The inset graph shows the relation $R_{90}/\phi \propto 1 + A\phi$. The circles (○) are calculated values from experimental data, and the solid line in this figure was calculated by substituting $a = 15.7$ nm, $\alpha = 1.45$ and $A = 11.7$. (b) The ϕ' dependence of D_z obtained from dynamic light scattering measurement. The circles (○) are the measured D_z, the solid line was drawn for extrapolating to $\phi' = 0$ and we obtained 25.5×10^{-12} m^2 s^{-1} as the extrapolated value for D_z.

We measured the excess Rayleigh ratio R_{90} (the scattering angle was fixed at 90°) at small ϕ' ($\phi' < 0.012$), and found a linear relation as shown in figure 3(a). Also dynamic light scattering measurements were performed at several small ϕ', and figure 3(b) represents the dependence of D_z on ϕ'. We obtained 25.5×10^{-12} m^2 s^{-1} extrapolating measured D_z to $\phi' = 0$ and the hydrodynamic diameter of the miniemulsion droplet a_z was determined as 18.5 nm.

We investigated the dependence of R_{90} on ϕ' at higher volume fraction and the result is presented in figure 4. Note that the maximum value of ϕ' is defined by the composition of a prepared miniemulsion (ϕ'_0). In this system ϕ_0 is equal to 0.2156. R_{90} increases linearly at low volume fraction, then flattens off, and passes a peak, to decrease monotonically with further increasing ϕ'. Similar curves were found by several authors [11–14] in microemulsion systems.

Consider a liquid dispersion of spherical droplets whose diameters are small compared with the incident light ($\lambda = 632.8$ nm). Light scattering arises from concentration fluctuations

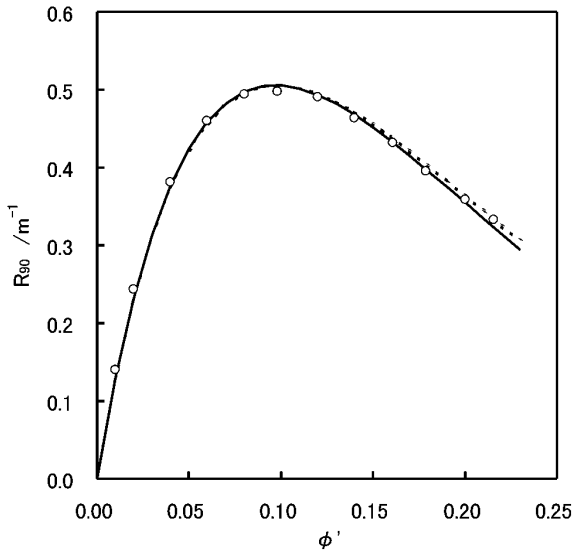

Figure 4. The ϕ' dependence of Rayleigh ratio R_{90} on at higher volume fraction ϕ'. ϕ' is varied from 0.01 to 0.2156. The circles (○) are the measured R_{90}, the solid line was calculated with equation (10) substituting $n_s = n_0 + 0.112\phi'$ and $\phi = \alpha\phi'$. As a result of non-linear least squares fitting, the values $\alpha = 1.35$ and $a = 15.5$ nm were obtained. The dashed line was calculated with equation (15) with $\gamma' = 0$ and the same values for α and a as above mentioned.

of droplets in a suspension. In this case Debye derived the following equation based on the fluctuation theory of Einstein [21]. For the incident light polarized perpendicularly with respect to the scattering plane, it is written as

$$R_\theta = \frac{4\pi^2 n_s^2}{\lambda^4}\left(\frac{\partial n_s}{\partial \rho}\right)^2 \rho \left(\frac{\partial}{\partial \rho}\frac{\Pi}{kT}\right)^{-1}. \tag{6}$$

Here R_θ is the excess Rayleigh ratio at the scattering angle θ, n_s is the refractive index of the mixture, λ is the wavelength of the incident light in vacuum, ρ is the particle number density and Π is the osmotic pressure at a temperature T with Boltzmann's constant k. Instead of ρ, we can use the volume fraction of dispersed droplets ϕ using the expression $\phi = \frac{1}{6}\rho\pi a^3$ where a is the droplet diameter. We supposed that in our case the miniemulsion droplets have the interaction potential due to hard sphere repulsion. Hence the main contribution to Π will be written as the compressibility in the Percus–Yevick approximation derived from a hard sphere fluid theory. Hiroike [22] and Baxter [23] proposed the following solution for Π/kT:

$$\frac{\Pi}{kT} = \frac{6}{\pi}\left\{\frac{\xi_0}{1-\xi_3} + \frac{3\xi_1\xi_2}{(1-\xi_3)^2} + \frac{3\xi_2^3}{(1-\xi_3)^3}\right\}. \tag{7}$$

If a monodisperse system with the diameter a is supposed, ξ_ν will be represented as

$$\xi_\nu = \frac{\pi}{6}\rho a^\nu = \phi a^{\nu-3}. \tag{8}$$

Substituting equation (8) into equation (7) yields the following expression for the osmotic compressibility:

$$\left(\frac{\partial}{\partial \phi}\frac{\Pi}{kT}\right)^{-1} = \frac{\pi}{6}a^3\frac{(1-\phi)^4}{(1+2\phi)^2}. \tag{9}$$

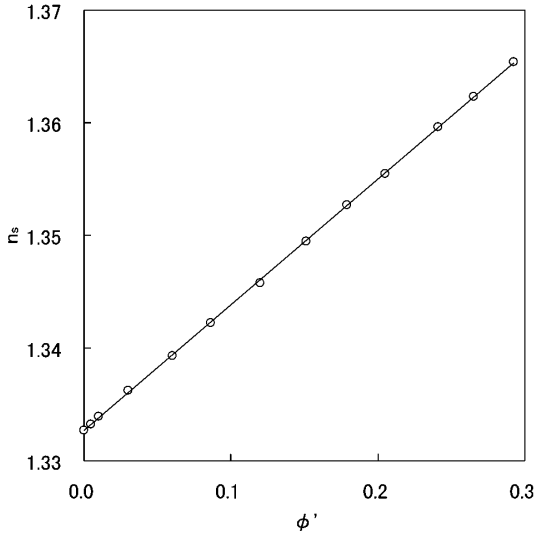

Figure 5. Dependence of the refractive index n_s on ϕ'. The circles (○) represent the experimental data and the solid line was calculated with $n_s = n_0 + 0.112\phi'$. The refractive index increment, $\partial n_s/\partial\phi'$, was determined as 0.112.

This is the solution of Wertheim [24] and Thiele [25] for the Percus–Yevick approximation. Vrij [26] applied the hard sphere fluid theory to light scattering of a concentrated multi-component system. Equations (6) and (9) give

$$R_\theta = \frac{2\pi^3 n_s^2}{3\lambda^4}\left(\frac{\partial n_s}{\partial\phi}\right)^2 a^3\phi\frac{(1-\phi)^4}{(1+2\phi)^2}. \tag{10}$$

In a miniemulsion system, we assume that the volume fraction of dispersed droplets ϕ will be proportional to the volume fraction of dispersed phase ϕ' as $\phi = \alpha\phi'$.

To apply equation (10), we must measure the refractive index increment of the obtained miniemulsion. Refractive indices of obtained miniemulsions n_s were measured using an Abbe refractometer adding water as the dispersion medium. We found that n_s was proportional to ϕ' in the whole concentration range as shown in figure 5. As a result of a least squares fit, we could obtain the following relationship: $n_s = n_0 + 0.112\phi'(\partial n_s/\partial\phi' = 0.112)$, where n_0 is the refractive index of water (1.3323).

Now equation (10) includes only two unknown parameters, a and α. The solid line in figure 4 indicates the fitting result by using equation (10) with $n_s = n_0 + 0.112\phi$ and $\phi = \alpha\phi'$. As the result of a non-linear least squares calculation, we obtained 1.35 as α and 15.5 nm as the hard sphere diameter of miniemulsion droplets a. We obtained 18.5 nm as the z-averaged hydrodynamic diameter a_z as mentioned above. Comparison of a and a_z shows that a is smaller than a_z. This difference is to be expected because a_z is estimated by the diffusive motion of a droplet while a is derived from the repulsive interaction between droplets. The ratio of the hydrodynamic diameter to the hard sphere one a_z/a is 1.19, and this is in agreement with another study for a microemulsion with nonionic surfactant [13]. For small ϕ', equation (10) is approximated by the following equation with the virial expansion for the osmotic compressibility Π/kT.

$$R_\theta = \frac{2\pi^3 n_0^2}{3\lambda^4}\left(\frac{\partial n_s}{\partial\phi}\right)^2 a^3\frac{\phi}{1+A\phi} \tag{11}$$

A being a virial coefficient. Equation (11) follows a conventional expression, $\phi/R_{90} \propto 1 + A\phi$ [12, 38]. The inset of figure 3 shows a plot of $K\phi'/R_{90}$ as a function of ϕ' for $\phi' < 0.1$, and we found a straight line with a positive value of A. K is deduced from equation (11), and the solid line in this figure was calculated by substituting $a = 15.7$ nm, $\alpha = 1.45$ and $A = 11.7$. We obtained a and α in agreement with those obtained in figure 4, but A is significantly larger than the reported values [12, 38]. In the present state, it is difficult to discuss the obtained values in detail, because of the error on ϕ'/R_{90}. The experimental value for A may be overestimated, but we consider that the agreement is qualitatively correct. At the region for $\phi' < 0.01$, we expect that this equation deduces a linear relation as $R_{90} \propto \phi'$ as shown in figure 3. In this case, the following equation is practically useful.

$$R_\theta = \frac{2\pi^3 n_0^2}{3\lambda^4}\left(\frac{\partial n_s}{\partial \phi}\right)^2 a^3\phi. \tag{12}$$

Using $\phi = \alpha\phi'$, therefore, we can evaluate a and α from $\partial R_{90}/\partial\phi$. As a fitting result, the values $\alpha = 1.35$ and $a = 15.6$ nm were obtained and the solid line represents equation (12) with those obtained values. We could confirm that equation (12) gives a good approximation and obtained values are compatible with those given in figure 4.

Some authors [11, 12] assumed that droplets behave as solutions with a potential which is the sum of a hard sphere repulsion Π_{HS}/kT and a small attractive term represented by a semi-empirical van der Waals-type attractive term Π_w/kT. They often use an expression for Π_{HS}/kT replacing equation (7) by the following equation.

$$\frac{\Pi_{HS}}{kT} = \frac{6}{a^3\pi}\frac{(1 + \phi + \phi^2 - \phi^3)}{(1-\phi)^3}. \tag{13}$$

This is the semi-empirical equation of Carnahan and Starling for the Percus–Yevick approximation [27]. For Π_w/kT, we can use the following expression as a perturbation term.

$$\frac{\Pi_w}{kT} = -\frac{1}{2}\gamma\phi^2. \tag{14}$$

Here γ is a constant determined by an interactive potential of van der Waals type. Combining equations (6), (13) and (14) makes it possible to obtain the following expression.

$$R_\theta = \frac{2\pi^3 n_s^2}{3\lambda^4}\left(\frac{\partial n_s}{\partial \phi}\right)^2 a^3\phi\left\{\frac{(1+2\phi)^2 - \phi^3(4-\phi)}{(1-\phi)^4} - \gamma'\phi\right\}^{-1} \tag{15}$$

and consider γ' as an adjustable parameter. This is in accordance with the apparent attractive interaction found from the positive value of γ' in equation (15). Fitting this equation to the variation of R_θ with ϕ' shown in figure 4, we found no significant value for γ' as a constant for the attractive term. The dashed line in figure 4 shows the fitting result using equation (15) with $\gamma' = 0$ and $\alpha = 1.35$. Hence we conclude that there is no great difference between equations (10) and (15) in this range of ϕ', i.e. the attractive potential between droplets in our system does not exist appreciably.

We performed dynamic light scattering measurements at higher ϕ'. The normalized diffusion coefficients of the faster and slower mode, D_f/D_0 and D_s/D_0, are given in figure 6. At lower volume fraction, $\phi' < 0.02$, the individual autocorrelation functions are well characterized by a single-exponential decay. In this case, only the D_f value was observed by means of a z-averaged diffusion coefficient on the cumulant analysis (equation (2)), and a correspondingly low value of $K_1/K_2^2 \cong 0.05$ was obtained. On the other hand, at a high volume fraction of the dispersion phase, the measured autocorrelation functions deviated from a single exponential. So obtained autocorrelation functions were analysed by using equation (4).

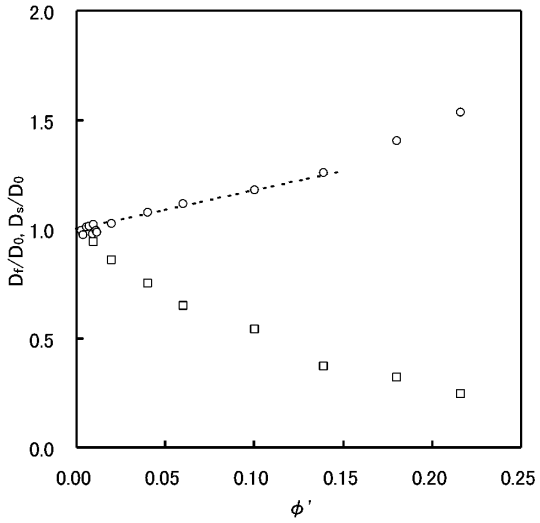

Figure 6. The dependence of D_f/D_0 and D_s/D_0 on ϕ'. Fitting equation (4) to the obtained autocorrelation function at each ϕ', D_f and D_s were estimated. Both of them are normalized by D_0, which is obtained by extrapolating D_f to ϕ'. At low volume fraction ($\phi' < 0.1$), only D_f was observed. The circles (○) represent D_f/D_0, and the squares (□) D_s/D_0. The dotted line was calculated by equation (16) substituting $\phi = 1.35\phi'$ and $k_{D,c} = 1.31$.

D_f and D_s were normalized with respect to the same value, $D_0 = 25.5 \times 10^{-12}$ m^2 s^{-1}, which is obtained by extrapolating D_z to $\phi' = 0$ (see figure 3(b)). The concentration dependence of D_f/D_0 and D_s/D_0, presented in figure 6, is very similar to that found in a colloidal hard sphere system [13, 38] when we consider that the obtained D_f and D_s represent the collective or mutual diffusion coefficient D_c and self- or tracer-diffusion coefficients D_t, respectively. According to Pusey *et al* [18], the faster decaying mode describes stochastic compression–dilution motions, and the slower one describes the exchange of different species in a colloidal hard sphere system. At low volume fraction of dispersed droplets ϕ, several authors give similar results for the dependence of D_c/D_0 and D_t/D_0 on ϕ taking only pairwise hydrodynamic interactions into account. The normalized collective diffusion coefficient D_c/D_0 and the self-diffusion coefficient D_t/D_0 are found to be

$$D_c/D_0 = 1 + k_{D,c}\phi \tag{16}$$

$$D_t/D_0 = 1 - k_{D,t}\phi. \tag{17}$$

Batchelor, for example, has given theoretically 1.45 and 1.83 (or 2.68) as $k_{D,c}$ and $k_{D,t}$, respectively [38, 39]. Fitting equation (16) to experimental data for D_f/D_0 with $\phi = 1.35\phi'$, we obtained 1.31 as $k_{D,c}$. Though this is slightly smaller than 1.45 as the theoretical value for $k_{D,c}$, it is quite similar to the $k_{D,c}$ value ($k_{D,c} = 1.3$) obtained experimentally by Olsson and Schurtenberger [13]. So we could conclude that D_f/D_0 observed in the dynamic light scattering experiment corresponds to the normalized collective diffusion coefficient.

In the case of the normalized diffusion coefficient for the slower mode D_s/D_0, a stronger volume fraction dependence is observed in the dilute regime than predicted by equation (17) with $k_{D,t} = 1.83$. Obtained D_s/D_0 values are well represented by a second-order polynomial: $D_s/D_0 = 1 - 4.3\phi + 5.6\phi^2$. Although the concentration dependence observed here is stronger than predicted by theory [38], its tendency is similar to that found in the other colloidal system [13, 37]. We therefore concluded that the observed slower decay mode D_s for concentrated

samples is probably associated with the self-diffusion of miniemulsion droplets. But due to the small amplitude and the other contribution to the obtained autocorrelation function (noise, polydispersity and so on), it is very difficult to discuss in detail at present.

3.3. Application of the relative intensity measurement techniques

In practice it is very useful to measure the variation of the relative scattering intensity $I^{rel}(q)$ with ϕ', because we can estimate it from the base line of the single-clipped, photoelectron-count autocorrelation function. If we fix the scattering angle at 90°, the Rayleigh ratio R_{90} will be represented by

$$R_{90} = \varphi n_s^2 \frac{I_{90}^{rel}}{I_0} \tag{18}$$

where φ is a constant dependent on instrumental conditions and I_0 is the intensity of the incident light. Substitution of equation (18) into equation (10) gives

$$I_{90}^{rel} = \frac{I_0}{\varphi} \frac{2\pi^3}{3\lambda^4} \left(\frac{\partial n_s}{\partial \phi} \right)^2 a^3 \phi \frac{(1-\phi)^4}{(1+2\phi)^2}. \tag{19}$$

In our instrument, it can be assumed that the intensity of the incident light I_0 is well stabilized and the droplet diameter a does not change in one step of measurements. The relative scattering intensity I_{90}^{rel} is therefore expressed as follows

$$I_{90}^{rel} = \varphi' \phi \frac{(1-\phi)^4}{(1+2\phi)^2} \tag{20}$$

with φ' as the adjustable parameter. Figure 7 shows the variations of I_{90}^{rel} as a function of volume fraction ϕ' for miniemulsions, which were prepared varying WOR from 4 to 10. Each solid line in figure 7 indicates the fitting result by equation (20). The data for preparations of miniemulsion and values for the adjustable parameter α are summarized in table 1. The coefficients α were varied from 1.01 to 1.33 with changing composition of the miniemulsion.

Table 1. Data for the fabrication of miniemulsions.

	Weight fraction					
WOR	Oil	Water	Surfactant	Quantity of surfactant (mol 1^{-1})	ϕ_0'	α
4	0.1439	0.7361	0.1200	0.2642	0.2924	1.010
5	0.1191	0.7609	0.1200	0.2660	0.2636	1.159
6	0.1007	0.7793	0.1200	0.2676	0.2433	1.255
7	0.0883	0.7917	0.1200	0.2686	0.2277	1.310
8	0.0782	0.8018	0.1200	0.2694	0.2156	1.329
9	0.0703	0.8097	0.1200	0.2700	0.2061	1.331
10	0.0638	0.8162	0.1200	0.2706	0.1983	1.328

3.4. Bound water on the dispersed droplets

It is important to discuss the obtained values for α, because we have no information for this parameter from a theoretical approach in spite of its significance on the fitting procedure. In general, it has been said that this underestimation of the dispersed phase volume fraction is concerned with the asymmetrical geometry of emulsion droplets, for example, the difference between the droplet diameter and the hard sphere one. As a result of Rayleigh ratio

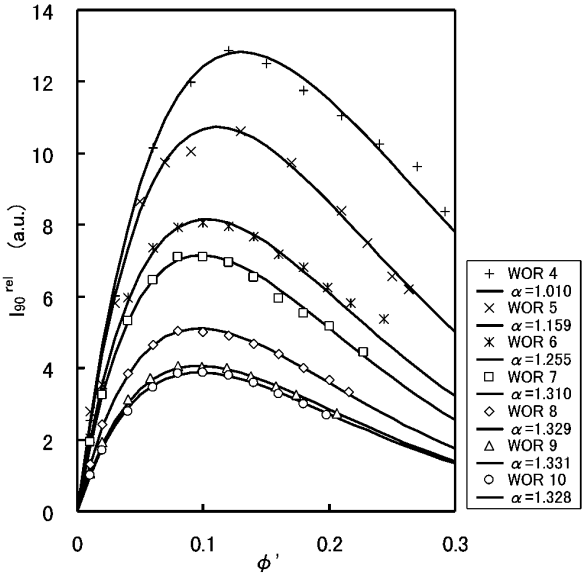

Figure 7. Variation of the relative scattering intensity I_{90}^{rel} with ϕ' for miniemulsions, which were prepared varying WOR from 4 to 10. Each solid line is the fitting result using equation (20) substituting $\phi = \alpha\phi'$. As a result, the obtained value for α varied from 1.01 to 1.33.

measurements, we found out that the hard sphere diameter is smaller than the hydrodynamic one. Moreover the result of the theoretical analysis represented in figure 4 indicated that the obtained miniemulsion is constituted of homogeneous droplets. It seems improbable, then, that these values for $\alpha > 1$ are explained from underestimation of droplet diameters and geometrical asymmetry.

Hence it may be reasonable to consider that these excess values of ϕ' are due to the error of estimation represented by equation (5). If we suppose that the surfactant volume V_s is calculated dividing mass by its density 0.998 in a miniemulsion phase, we must consider the value $\alpha > 1$ indicates the underestimation of the numerator of equation (5). We assume that ϕ is calculated by

$$\phi = \frac{V_o + V_s + V_{bw}}{V_o + V_s + V_w}. \tag{21}$$

Here V_{bw} indicates the volume of bound water on O/W miniemulsion droplets.

From α, ϕ' and the hydrodynamic diameter a_z measured by dynamic light scattering measurements, it is possible to calculate V_{bw}, the total surface area S_0, the number of miniemulsion droplets n_0 and the minimum surface area per molecule A_m^s (see table 2). We could find the obtained values for A_m^s in good agreement with the reported value of 0.573 nm^2 for the minimum surface area per molecule for $C_{12}EO_7$ at the aqueous solution/air interface [28]. Figure 8 shows the variation of V_{bw} as a function of ϕ_0'. This curve implies that the amount of bound water is concerned with the composition of the system.

3.5. A role of bound water for the formation of homogeneous miniemulsion phases

It has been suggested that the excellent solubility of poly(ethylene oxide), PEO, in water is due to some specific hydrogen-bond formation between the ethylene oxide units of PEO and water molecules [29–31]. On the other hand, it has been indicated equally that the hydrophobic

Table 2. Results of data analysis.

WOR	a_z (nm)	ϕ_0	S_0 (m^2 cm^{-3})	n_0 (droplets cm^{-3})	A_m^s (nm^2)	V_{bw}	N_m^{bw}
4	22.9	0.2953	77.4	4.697×10^{16}	0.487	0.0032	0.67
5	21.7	0.3055	84.5	5.710×10^{16}	0.528	0.0471	9.83
6	20.7	0.3053	88.5	6.575×10^{16}	0.549	0.0713	14.8
7	19.8	0.2982	90.4	7.339×10^{16}	0.559	0.0800	16.5
8	17.4	0.2865	98.8	1.039×10^{17}	0.609	0.0804	16.6
9	16.1	0.2743	102.2	1.255×10^{17}	0.629	0.0773	15.5
10	14.8	0.2633	106.8	1.551×10^{17}	0.655	0.0737	15.1

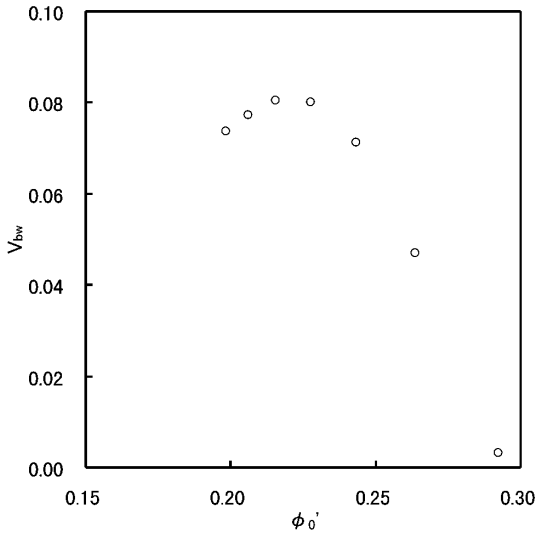

Figure 8. Variation of V_{bw} as a function of ϕ_0' estimated by using equation (21) with each α value listed in table 1.

interaction plays an important role for the accommodation of ethylene oxide chains in water, which originates from the increased structuring water around the ethylene oxide chains [32, 33]. In a similar way, these effects will be expected in the case of nonionic surfactants, especially poly(ethylene oxide) surfactants [34]. According to these suggestions, it seems plausible that the volume of bound water in our system is due to the interaction between water molecules and ethylene oxide chains as the hydrophilic head group of nonionic surfactants. In this case we can derive the average number of bound water molecules per ethylene oxide chain N_m^{bw} as shown in table 2. Though it is difficult to evaluate an accurate value for N_m^{bw} because V_s must be changed in an emulsion phase, obtained values for N_m^{bw} are feasible in our estimation.

Many authors have described the number of 'bound' water molecules per ethylene oxide repeat unit theoretically and experimentally [29–34]. ^2H and ^{17}O NMR measurements revealed that the water mobility of bound water in the PEO hydration phase is retarded by a factor of 2 to 5 compared with that of 'free' water in the bulk [29]. Moreover NMR measurements of the chemical shifts of the CH_2 and OH protons suggest that a hydrated complex is formed comprising three water molecules per ethylene oxide unit [35]. Quasi-elastic neutron scattering measurements supply evidence that strongly supports the existence of a 1:1 hydrated complex [30]. From differential scanning calorimetry measurement, it was concluded that two water

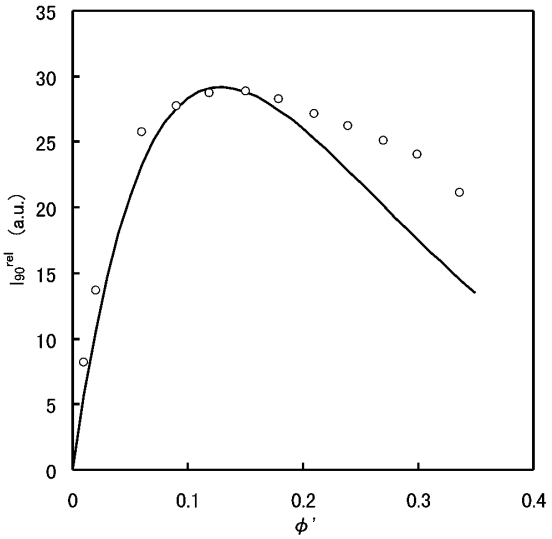

Figure 9. Variation of I_{90}^{rel} with ϕ' for the emulsion, of which WOR is 3 and the weight fraction of surfactant is 0.12, prepared by the same thermal protocol as described in section 3.1. The obtained phase was monophasic, but it was cloudy compared with the miniemulsion phase. The circles (○) are measured values; the solid line was calculated with equation (20) with the values for α as 1.000.

molecules per ethylene oxide unit are tightly bound to the PEO chain [32]. Several theoretical approaches have suggested that physical bond formation between PEO segments and water molecules [36] or the structuring of water around PEO segments [33] may be a major cause of reentrant phase separation in the PEO–water system. In miniemulsions we used $C_{12}EO_7$ as the nonionic surfactant, which has seven ethylene oxide units. So the average number of bound water molecules per ethylene oxide unit is varied from 0.34 to 2.37. This is in agreement with the above-mentioned experimental and theoretical results.

In figure 8, it is clear that V_{bw} depends on ϕ_0'. The experimental curve for V_{bw} is seen to have a peak and decrease monotonically with increasing ϕ_0' at $\phi_0' > 0.22$. This tendency may be concerned with the microscopic geometry of miniemulsion droplets, PIT of each composition of miniemulsion, the formation process of the miniemulsion and so on. At present, however, we have no experimental data that can explain this tendency. We postpone the question until more detailed data are obtained.

The experimental result in figure 8 implies that there is no positive value of V_{bw} when WOR is smaller than 3. This region corresponds to the condition that we could no longer obtain a translucent O/W emulsion phase in this system. We obtained Winsor's phase I when WOR is equal to 1 and 2, and a monophasic but relatively opaque emulsion was obtained when WOR is 3. The variation of I_{90}^{rel} with ϕ_0' for a WOR of 3 is represented in figure 9. This experimental curve shows an anomalous behaviour and we could not adjust equation (20) to these data (see the solid line in figure 9). So we conclude that the microstructure of the obtained emulsion phase may be quite different from the other one. This indicates the fact that bound water will play an important role for the formation or stabilization of a homogeneous O/W miniemulsion phase; in other words, a positive value for V_{bw} allows us to obtain a homogeneous O/W miniemulsion phase. Also, we remarked that it is possible to find the maximum value of the variation of V_{bw} with WOR, i.e. an optimal composition for a homogeneous miniemulsion phase will exist. This may suggest equally an important role of the bound water in its formation.

4. Conclusion

We investigated the hard sphere interaction of O/W miniemulsion droplets in the ternary system of water/oil/nonionic surfactant by using light scattering measurement techniques. First we elucidated the role of phase inversion temperature to obtain translucent O/W miniemulsion phases. It was shown that the variation of the scattering light intensity with the dispersed phase volume fraction ϕ' can be analysed by the theoretical equation derived from a hard sphere fluid theory with the Percus–Yevick approximation. We found out that the obtained O/W miniemulsion droplets have a hard sphere interaction potential between them and this system is homogeneous. At the composition for which WOR is 8 and the weight fraction of surfactant is 0.12, the hard sphere diameter a measured by Rayleigh ratio measurements was 15.5 nm, and the z-average hydrodynamic diameter a_z evaluated by dynamic light scattering measurements was 18.4 nm. We found that the ratio of the hydrodynamic diameter to the hard sphere diameter is 1.19 and the volume fraction of dispersed droplets is given by $\phi = 1.35\phi'$.

We also applied relative scattering intensity measurements as a practical technique, and proposed a simple equation with two adjustable parameters for the data analysis. Measuring the variation of the scattering intensity with ϕ' in miniemulsions of various WOR, it was found that the $\phi\phi'$ ratio varied from 1.01 to 1.33. It was therefore clarified that the volume fraction of dispersed phase ϕ' is obviously underestimated compared with ϕ. If it is assumed that bound water exists around ethylene oxide chains of nonionic surfactant, we could estimate the number of bound waters per ethylene oxide chain, which varied from 0.67 to 16.6. It was clear that the volume of bound water V_{bw} depends on the dispersed phase volume fraction at the preparation for miniemulsion ϕ'_0. The obtained experimental curve for V_{bw} is seen to have a peak and decrease monotonically with increasing ϕ'_0 at $\phi'_0 > 0.22$. This experimental curve implies that V_{bw} becomes negative at $\phi'_0 > 0.27$. When we prepared a miniemulsion with a ϕ'_0 value which corresponds to a negative value for V_{bw}, we could not obtain a translucent and homogeneous O/W miniemulsion phase. Hence we concluded that this suggests the fact that the bound water plays an important role in obtaining a homogeneous O/W miniemulsion phase.

References

[1] Everett D H 1988 *Basic Principles of Colloid Science* (Cambridge: Royal Society of Chemistry)
Rosen M J 1989 *Surfactants and Interfacial Phenomena* (New York: Wiley)
[2] Ushiki H 1999 *Applied Fluorescence in Chemistry, Biology, and Medicine* ed B Strehmel, S Scharader and H Seifert (Berlin: Springer) pp 325–70
[3] Ushiki H 1992 *Rep. Prog. Polym. Phys. Japan* **35** 419
[4] Davis H T 1994 *Colloids Surf.* A **91** 9
[5] Lee H, Pober R and Calvert P 1986 *J. Colloid Interface Sci.* **110** 144
[6] Ottewill R H and Rastogi M C 1960 *Trans. Faraday Soc.* **56** 866
Ottewill R H and Rastogi M C 1960 *Trans. Faraday Soc.* **56** 880
[7] Ottewill R H and Walker T 1968 *Kolloid-Z.Z. Polym.* **227** 108
[8] Sing A J F 1997 *PhD Dissertation* University of Pau
[9] Sing A J F, Grasiaa A, Lachaise J, Brochette P and Salager J L 1999 *Colloids Surf.* A **152** 31
[10] Percus J K and Yevick G J 1957 *Phys. Rev.* **110** 1
[11] Agterof W G M, van Zomeren J A J and Vrij A 1976 *Chem. Phys. Lett.* **43** 363
[12] Cazabat A M, Langevin D and Pouchlon A 1980 *J. Colloid Interface Sci.* **73** 1
[13] Olsson U and Schurtenberger P 1993 *Langmuir* **9** 3389
[14] Kahlweit M, Strey R, Sottmann T, Busse G, Faulhaber B and J Jen 1997 *Langmuir* **13** 2670
[15] Shinoda K and Saito H 1968 *J. Colloid Interface Sci.* **26** 70
Shinoda K and Saito H 1969 *J. Colloid Interface Sci.* **30** 258
[16] See for instance, Berne B J and Pecora R 1976 *Dynamic Light Scattering* (New York: Wiley)

[17] Koppel D E 1972 *J. Chem. Phys.* **57** 4814
[18] Pusey P N, Fijnaut H M and Vrij A 1982 *J. Chem. Phys.* **77** 4270
[19] Nakagawa T and Oyanagi Y 1982 *Saishou Nijou-hou niyoru Jikken-Data Kaiseki* (Tokyo: Daigaku Syuppan-kai)
Tsunomori F and Ushiki H 1996 *Polym. J.* **28** 576
Tsunomori F and Ushiki H 1996 *Polym. J.* **28** 582
Tsunomori F and Ushiki H 1996 *Polym. J.* **28** 588
[20] Shinoda K and Arai H 1964 *J. Phys. Chem.* **68** 3485
[21] Debye P 1943 *J. Appl. Phys.* **15** 338
Debye P 1947 *J. Phys. Chem.* **51** 18
[22] Hiroike K 1969 *J. Phys. Soc. Japan* **27** 1415
[23] Baxter R J 1970 *J. Chem. Phys.* **52** 4559
[24] Wertheim M S 1963 *Phys. Rev. Lett.* **10** 321
[25] Thiele E 1963 *J. Chem. Phys.* **39** 474
[26] Vrij A 1978 *J. Chem. Phys.* **69** 1742
Vrij A 1982 *J. Colloid Interface Sci.* **90** 110
[27] Carnahan N F and Starling K E 1969 *J. Chem. Phys.* **51** 635
[28] Rosen M J, Cohen A W, Dahanayake M and Hua X 1982 *J. Phys. Chem.* **86** 541
[29] Breen J, Huis D, de Bleijser J and Leyte J C 1981 *J. Chem. Soc. Faraday Trans. I* **84** 293
[30] Maconnachie A, Vasudevan P and Allen G 1978 *Polymer* **19** 33
[31] Blandamer M J, Fox M F, Powell E and Stafford J W 1969 *Makromol. Chem.* **124** 222
[32] de Vringer T, Joosten J G H and Junginger H E 1986 *Colloid Polym. Sci.* **264** 623
[33] Kjellander R and Florin E 1981 *J. Chem. Soc. Faraday Trans. I* **77** 2053
[34] Kjellander R 1982 *J. Chem. Soc. Faraday Trans. II* **78** 2025
[35] Liu K J 1968 *Macromolecules* **1** 213
Liu K J and Parsons J L 1969 *Macromolecules* **2** 5293
[36] Matsuyama A and Tanaka F 1990 *Phys. Rev. Lett.* **65** 75
[37] van Megen W and Underwood S M 1989 *J. Chem. Phys.* **91** 552
[38] Kops-Werkhoven M M and Fijnaut H M 1981 *J. Chem. Phys.* **74** 1618
Kops-Werkhoven M M and Fijnaut H M 1982 *J. Chem. Phys.* **77** 2242
Kops-Werkhoven M M, Pathmamanoharan C, Vrij A and Fijnaut H M 1982 *J. Chem. Phys.* **77** 5913
[39] Batchelor G K 1972 *J. Fluid Mech.* **52** 245
Batchelor G K 1976 *J. Fluid Mech.* **74** 1